Biosensors and Bioelectronics 40 (2013) 219–226

Contents lists available at SciVerse ScienceDirect

Biosensors and Bioelectronics

journal homepage: www.elsevier.com/locate/bios

The effect of uniform capture molecule orientation on biosensor sensitivity: Dependence on analyte properties

Anke K. Trilling [a,b], Michiel M. Harmsen [c], Vincent J.B. Ruigrok [d], Han Zuilhof [b,e], Jules Beekwilder [a,*]

[a] Plant Research International, P.O. Box 16, 6700 AP Wageningen, The Netherlands
[b] Laboratory of Organic Chemistry of Wageningen University, P.O. Box 8026, 6700 EG Wageningen, The Netherlands
[c] Central Veterinary Institute of Wageningen University, P.O. Box 65, 8200 AB Lelystad, The Netherlands
[d] Laboratory of Microbiology of Wageningen University, Dreijenplein 10, 6703 HB Wageningen, The Netherlands
[e] Department of Chemical and Materials Engineering of King Abdulaziz University, Jeddah, Saudi Arabia

ARTICLE INFO

Available online 23 July 2012

Keywords:
Surface plasmon resonance
Llama heavy-chain antibodies
Site-specific biotinylation
Orientation
Foot-and-mouth disease virus
Tuberculosis

ABSTRACT

Uniform orientation of capture molecules on biosensors has been reported to increase sensitivity. Here it is investigated which analyte properties contribute to sensitivity by orientation. Orientation of capture molecules on biosensors was investigated using variable domains of llama heavy-chain antibodies (VHHs) as capture molecule, and a surface plasmon resonance (SPR) chip as biosensor. Two VHHs were tested in this study: one recognizing foot-and-mouth disease virus (FMDV) and another recognizing the 16 kDa heat-shock protein of *Mycobacterium tuberculosis*. SPR chips with randomly immobilized biotinylated VHHs were compared to streptavidin-coated SPR chips, on which similar quantities of oriented biotinylated VHHs were non-covalently immobilized. Analytes that differ in molecular weight, epitope number and epitope affinity were compared using the FMDV-recognizing VHH. When binding of intact FMDV particles (146 S; 8200 kDa) or pentameric FMDV coat protein aggregates (12 S; 282 kDa) was detected, a modest (1–2-fold) increase in sensitivity was observed. When a 26-residue peptide (3 kDa) containing the epitope for VHH recognition was tested, much larger effects of capture molecule orientation (14-fold) on signal were observed. A 20–227-fold improvement was also observed when the epitope peptide was covalently linked to bovine serum albumin (67 kDa) or R-phycoerythrin (240 kDa). The results indicate that orientation of the capture molecule hardly affects high-affinity interactions, while it leads to strong improvements in sensitivity for lower-affinity interactions.

1. Introduction

The ongoing need for miniaturization of diagnostic elements such as biosensors implies that space for the actual detection components will be strongly limited. To compensate for this reduction in surface area, the biological detection elements need to be optimized. This optimization may include correct and uniform orientation at high density, in order to enhance analyte binding and to increase sensitivity of the device (Seo et al., 2011; Tajima et al., 2011; Vashist et al., 2011; Zeng et al., 2012).

Sensitivity and specificity of biosensors depend on high-affinity and specific capture molecules. Antibodies are generally used as biological capture molecules in immunoassays such as ELISAs, as they form highly specific and high affinity interactions. Nowadays, many biosensors deploy antibodies as capture molecules (Holford et al., 2012; Zeng et al., 2012). One of the challenges faced in the design of multiplex biosensors is to reach, on a single sensor, a high sensitivity for a large number of targets. One solution may be to achieve a high number of binding units per mm^2, ideally all oriented in the same way. Conventional antibodies, with a typical molecular weight of 150 kDa and a size of $14 \times 9 \times 4\ nm^3$ (Sarma et al., 1971), are big in size. Due to the presence of many exposed reactive residues, site-specific functionalization of these molecules is challenging. Therefore, the truly oriented printing of antibodies on biosensor surfaces is not straightforward. To deploy antibody-like molecules of smaller size, diverse formats were exploited for use in biosensors (Zeng et al., 2012). One such format is the variable domain of heavy-chain antibodies of llamas, which are naturally devoid of light chain (VHH). VHHs offer advantages in terms of size (Dumoulin et al., 2002), stability (Saerens et al., 2008), expression yields (Thomassen et al., 2002) and ease in protein engineering.

Various covalent and non-covalent immobilization strategies for proteins have been employed to attach capture molecules to a surface (Hernandez and Fernandez-Lafuente, 2011). The extraordinarily high affinity of streptavidin to biotin was frequently used to immobilize biotinylated antibodies on streptavidin-modified surfaces (Cho et al., 2007; Saerens et al., 2005). Site-specific in vivo biotinylation at the C-terminus of VHHs can be achieved by introducing a specific tag sequence, which is biotinylated by the BirA enzyme of *Escherichia coli* (Beckett et al., 1999).

* Corresponding author. Tel.: +31 317 480979; fax: +31 317 418094.
E-mail address: jules.beekwilder@wur.nl (J. Beekwilder).

0956-5663/$ - see front matter © 2012 Elsevier B.V. All rights reserved.
http://dx.doi.org/10.1016/j.bios.2012.07.027

This approach can be used for the orientation of VHH capture molecules onto surfaces. Such orientation provides potential for higher binding capacity of the analyte: whereas in random immobilization, analyte-recognition sites are poorly exposed to the surface, orientation can be tuned for maximal exposure of the capture molecule to the analyte (Fig. 1). Techniques like circular dichroism spectroscopy (Le Brun et al., 2011), total internal reflection ellipsometry (Balevicius et al., 2011), time-of-flight secondary ion mass spectrometry (Baio et al., 2011; Cho et al., 2011; Park et al., 2011) and atomic force microscopy (Farris and McDonald, 2011) were used to display the antibody orientation in a direct manner. As an alternative, and in fact more directly linked to the application, the signal increase of oriented antibodies can be used as indirect method to determine the successful orientation of antibodies. Increased sensitivity after orientation of antibodies is well documented (Cho et al., 2009; Klonisch et al., 1996; Peluso et al., 2003; Shen et al., 2011; Song et al., 2012; Vareiro et al., 2005). However, reported improvements are highly variable, and the impact of analyte properties on the detection limit in uniformly and randomly oriented capture molecules has not been reported.

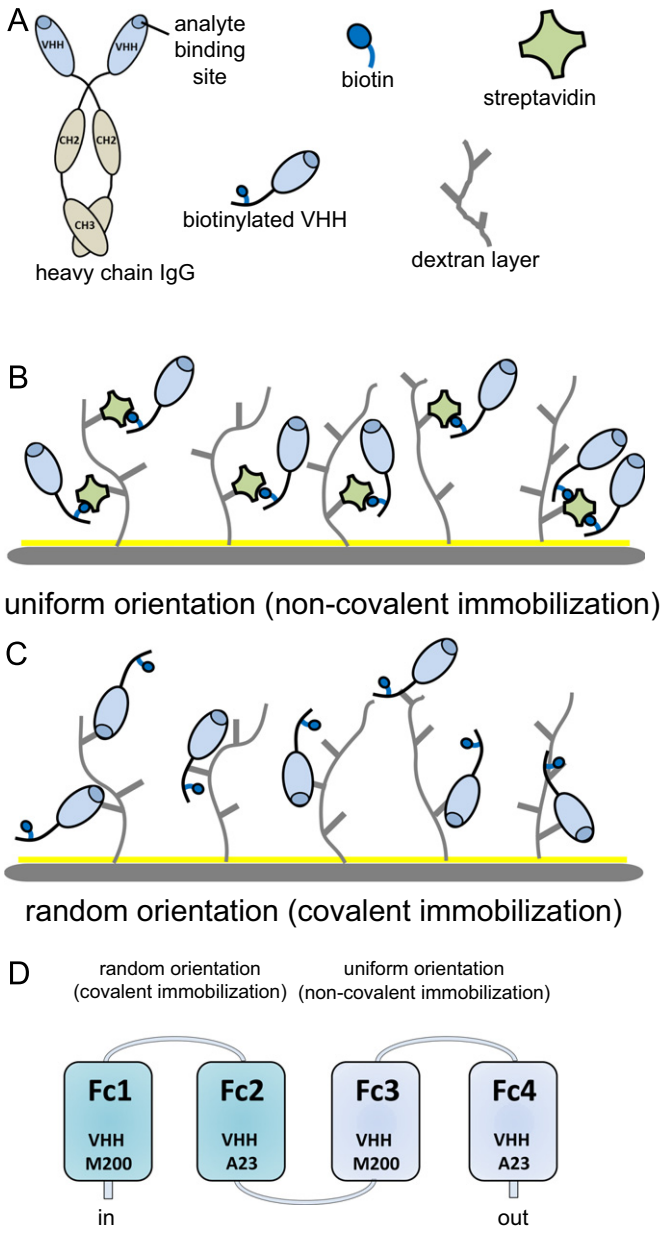

Fig. 1. Schematic illustration of immobilized VHHs on a carboxymethyl dextran sensor chip (CM5). A: heavy-chain antibody IgG. Biotin was introduced at the C-terminus of the VHH, the opposite site of the analyte binding site. B: biotinylated VHHs non-covalently immobilized in a uniform orientation onto streptavidin-coated CM5 sensor chips. C: biotinylated VHHs covalently coupled in random orientation via the amine groups onto CM5 sensor chips. VHHs can be immobilized via the ε-amines, present in lysine side chains, or via the α-amine, present at the N-terminus of the protein. D: set-up of SPR sensor chip with 4 flow channels (Fc).VHH M200 was immobilized randomly oriented in Fc1 and uniformly oriented in Fc3 and VHH A23 was immobilized randomly oriented in Fc2 and uniformly oriented in Fc4. For measurements analyte was injected in series over Fc1, Fc2, Fc3 and Fc4.

In a previous study we showed the use of VHHs as capture molecule using surface plasmon resonance (SPR) (Trilling et al., 2011). In the current study, as a next step, two different VHHs were engineered using a tag sequence to obtain site-specific biotinylation (Beckett et al., 1999). These two tailor-made VHHs were subsequently immobilized on the sensor surface in two ways: in a randomly oriented, covalent manner (via coupling of amine moieties with the activated surface), and in a uniformly oriented, non-covalent way by the use of streptavidin-coated surfaces and the non-covalent biotin-streptavidin interaction. The sensitivity of the resulting surfaces was studied towards a wide range of analytes. This has led to a high sensitivity enhancement upon uniform orientation (up to factor 227). Finally, we will develop a hypothesis to understand which analyte properties seem to govern the effects of uniform capture molecule orientation on the sensitivity of the sensor, with a specific focus on analyte molecular weight, avidity and specifically affinity.

2. Material and methods

2.1. Analytes of VHH

VHH A23 (Genbank accession no. JN234011.1) detects the 16 kDa heat-shock protein of *Mycobacterium tuberculosis*, and was characterized before (Trilling et al., 2011). Mycobacterium lysates (*M. tuberculosis*1, *M. tuberculosis*27 and *M. smegmatis*, Royal Tropical Institute, Amsterdam, The Netherlands) were prepared as described before (Trilling et al., 2011).

VHH M200 is specific for the GH-loop of structural protein VP1 of foot-and-mouth disease virus (FDMV) (Harmsen et al., 2007b). FMDV analyte and 12S particles derived thereof by acidification were prepared as described before (Harmsen et al., 2007a; Harmsen et al., 2011). Peptide PAT49 (acetyl-YGDGTVANVRGDLQVLAQKAAR-ALPC-amide), corresponding to amino acid residues 136–160 of the GH-loop of the FMDV O1 Manisa strain was purchased from Peptide 2.0 (Chantilly, US). Peptide PAT49 was coupled with the additional C-terminal cysteine residue to maleimide-activated bovine serum albumin (BSA) and R-phycoerythrin (Innova Biosciences Ltd., UK). Maleimide-activated protein was reacted overnight at room temperature in phosphate-buffered saline (PBS) pH 7.2 with peptide PAT49 in a 1:20 and 1:5 M ratio, resulting in BSA–PAT49 and R-phycoerythrin–PAT49. To subsequently block unreacted maleimide moieties, cysteine was added in excess. BSA–PAT49 and R-phycoerythrin–PAT49 were purified on Superdex 200 (GE Healthcare, Uppsala, Sweden) and concentrated using filter tubes (Millipore, The Netherlands). Protein concentrations were determined with the Pierce 660 nm Protein assay using NanoDrop 1000 and albumin as reference protein for the standard curve.

2.2. Biotinylation of VHH

VHHs are present in a vector for periplasmic VHH expression under control of the T7 promoter, based on the backbone of the pRSET-A vector (Invitrogen, The Netherlands). The C-terminus of

the VHH was fused to an AviTag (GLNDIFEAQKIEWHE) (Avidity, LLC, Colorado) for in vivo biotinylation along with a His-6 tag for purification purposes followed by a stop codon. Plasmid pBirAcm, an IPTG inducible plasmid containing the BirA gene engineered into pACYC184 (Avidity), was transformed to *E. coli* BL21-AI and used for in vivo biotinylation. Expression was performed according to Cloutier et al. (Cloutier et al., 2000), purification was performed as reported before (Trilling et al., 2011).

2.3. Western blot analysis

Purified biotinylated VHH (1.5 μg) was first boiled and reduced in buffer and electrophoresed on a 15% SDS-PAGE gel. For Western blotting, proteins were transferred from gel to a nitrocellulose membrane (Trans-Blot, Bio-Rad, Hercules, CA). These membranes were subsequently blocked overnight at room temperature in 2% milk in PBS pH 9.0 on a shaker, and then incubated with either anti-His6-Peroxidase (1:4000 in 2% (w/v) milk in PBS pH 9.0, Roche, Mannheim, Germany) or streptavidin-Peroxidase (1:5000 in 2% (w/v) milk in PBS pH 9.0, Roche) for 1 h at room temperature on a shaker. Next, the membranes were washed once with 2% milk in PBS pH 9.0, followed by two washing steps with PBS pH 9.0 containing 0.1% Tween 20 and two washing steps with PBS pH 9.0. Specific binding was detected with 3,3',5,5'-tetramethylbenzidine (TMB) liquid substrate system for membranes (Sigma-Aldrich, The Netherlands). The molecular weight standard was Page Ruler Prestained Protein ladder (Thermo Scientific).

2.4. Surface plasmon resonance (SPR)

Carboxymethyl dextran sensor chips (CM5), HBS-EP buffer (pH 7.4, consisting of 10 mM 4-(2-hydroxyethyl)piperazine-1-ethanesulfonic acid, 150 mM sodium chloride, 3 mM ethylenediaminetetraacetic acid, 0.005% v/v surfactant polysorbate 20), the amine coupling kit (containing 0.1 M N-hydroxysuccinimide (NHS), 0.4 M 1-ethyl-3-(3-dimethylaminopropyl)carbodiimide hydrochloride (EDC) and 1 M ethanolamine hydrochloride (pH 8.5)) were purchased from GE Healthcare (Uppsala, Sweden).

Oriented immobilization: In a Biacore 3000 streptavidin was immobilized onto a CM5 surface by the use of the amine coupling kit and the "Aim-for–Immobilization" wizard as present in the Biacore 3000 control software. To this aim the biosensor surface was activated by injecting (35 μL at a flow rate of 5 μL/min) a mixture of EDC and NHS (1:1; v/v) into flow channels (Fc3 and Fc4). Then streptavidin (50 μg/mL in coupling buffer [10 mM sodium acetate, pH 4.0]) was injected and bound to the activated carboxymethylated dextran surface via its primary amine groups, aiming for an immobilization level of 4000 response units (RU). After coupling, the remaining active groups were blocked with ethanolamine hydrochloride (1 M, 35 μL at a flow rate of 5 μL/min). VHHs with a site-specifically attached biotin label were subsequently captured onto a streptavidin surface in flow channels (Fc3 and Fc4) (Fig. 1B) in an oriented manner. To non-covalently immobilize biotinylated VHHs on the streptavidin surface 10 μL biotinylated VHH M200 (50 μg/mL in HBS-EP buffer) was injected at a flow of 5 μL/min over Fc3 resulting in 3183 ± 638 RU. The same procedure was repeated for biotinylated VHH A23 on Fc4 resulting in 3125 ± 423 RU.

Random orientation: Biotinylated VHHs were immobilized onto a CM5 surface by the use of the amine coupling kit and the "Aim-for–Immobilization" wizard. The biosensor surface was activated by injecting (35 μL at a flow rate of 5 μL/min) a mixture of EDC and NHS (1:1, v/v) into flow channels (Fc1 and Fc2) (Fig. 1C). Then biotinylated VHH (50 μg/mL in coupling buffer) was injected and bound to the activated carboxymethylated dextran surface via its primary amine groups, aiming for an immobilization level of 3500 response units (RU). After coupling, the remaining active groups were blocked with ethanolamine hydrochloride (1 M, 35 μL at a flow rate of 5 μL/min). Immobilization of biotinylated VHH M200 on Fc1 resulted in 3420 ± 317 RU, of biotinylated VHH A23 on Fc2 in 3344 ± 262 RU.

The Biacore 3000 SPR machine was operated at a constant temperature of 25 °C and a flow of 10 μL/min. 50 μL analyte preparations in HBS-EP buffer, each of different analyte concentration, were injected over the four serially connected flow channels. Regeneration of the sensor surface was achieved with 5 μL of a 10 mM hydrogen chloride solution (HCl), which was passed through at a flow rate of 10 μL/min after each run. Data points were measured 30 s after injection end at time point 400.5 s. All sensorgrams were referenced by subtracting the signal from the reference flow channel and were evaluated using the BIAevaluation software.

2.5. Affinity measurements

Affinity of VHH M200 to peptide PAT49, FMDV and 12S was determined by ELISA, using a competition assay as done before (Harmsen et al., 2008). Shortly, 100 μL of a 50 nM VHH M200 solution was pre-incubated overnight with a dilution series of analyte at room temperature in 2% milk PBS pH 9.0. Pre-incubated VHH M200 was then transferred to a plate coated with a low density of analyte (FMDV: 1 μg/mL total protein corresponding to 0.2 μg/mL FMDV, 12S particle: 1 μg/mL total protein corresponding to 0.2 μg/mL 12S particle and peptide PAT49: 0.5 μg/mL) in 50 mM carbonate buffer pH 9.6. VHH M200 bound to the plate was detected using anti-His6-Peroxidase (1:4000 in 2% (w/v) milk in PBS pH 9.0, Roche). Subsequently HRP activity was determined by adding 1-StepTM Ultra TMB-ELISA substrate (Pierce, Rockford, IL). The reaction was allowed to proceed in the dark for 30 min and then stopped with 1 M sulphuric acid and the OD was measured at 415 nm in a microtiter plate-reader (TECAN Spectra-Fluor Microplate Reader).

3. Results

3.1. Biotinylated VHHs

Two VHHs, M200 and A23 were used. A strategy was used to allow site-specific biotinylation of the VHHs, without affecting their binding properties. The X-ray structure of VHHs reveals that the C-terminus is positioned at the opposite of the analyte-binding site (Renisio et al., 2002; Spinelli et al., 1996), and biotinylation at the C-terminus is therefore not expected to interfere with analyte binding. Therefore, both VHH genes were fused to a C-terminal AviTag, followed by a His-6 tag for purification. Both VHHs were subsequently produced in *E. coli*, where it was co-expressed with the BirA enzyme. After Ni-NTA purification of the VHHs from the *E. coli* lysate, VHHs were analyzed using Western blotting (Fig. 2A). The produced proteins displayed a single band on the western blot, either detected by an anti-His6-Peroxidase antibody, or by Streptavidin-Peroxidase, indicating that the major biotinylated protein in the capture molecule preparation was the VHH.

3.2. Analyte collection

VHH A23 detects the 16 kDa heat-shock protein in *Mycobacterium tuberculosis*. Two lysates of *M. tuberculosis* (*M. tuberculosis*1, *M. tuberculosis*27) were used, which positively react to A23, and compared to a lysate of *M. smegmatis* which is not recognized by A23 (Trilling et al., 2011).

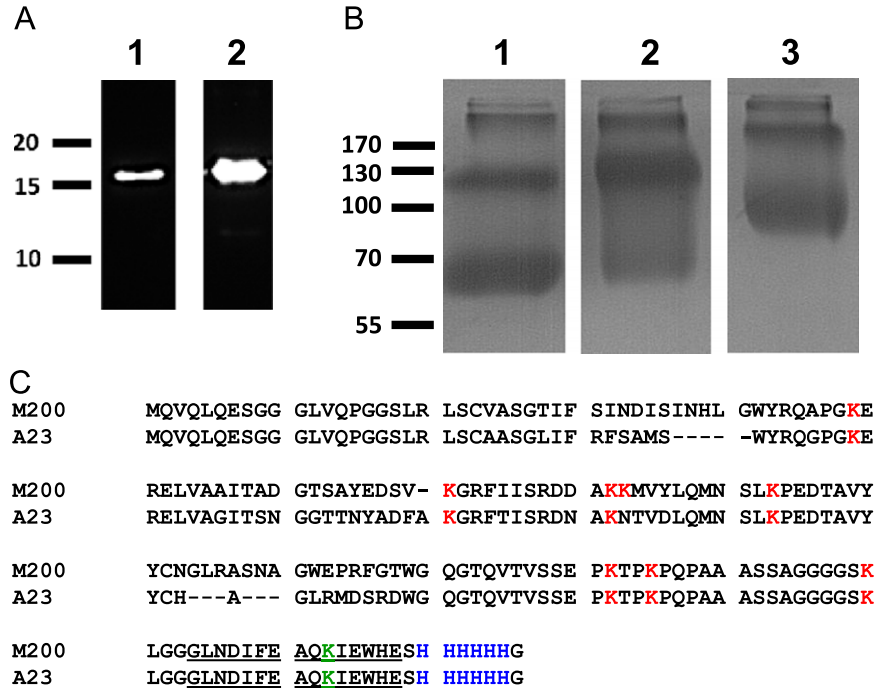

Fig. 2. Analysis of BSA–PAT49 and purified VHHs. A: western blot analysis of biotinylated M200. 1.5 μg of Ni-resin-purified VHH was used for separation on SDS-PAGE gel. Lane 1: detected with anti-His6-Peroxidase. Lane 2: detected with Streptavidin-Peroxidase. B: evaluation of molecular weight shift for BSA upon coupling with PAT49 on SDS-PAGE. Lane 1: maleimide-activated BSA starting material. Lane 2: BSA–PAT49 product after coupling reaction of starting material with 5 M equivalents peptide PAT49 and blocking of unreacted maleimide-moieties with cysteine, not purified. Lane3: BSA–PAT49 product after coupling reaction of starting material with 20 M equivalents peptide PAT49 and blocking of unreacted maleimide-moieties with cysteine, not purified. Indicated are the positions of relevant size markers in kDa. C: aligned amino acid sequences of VHH M200 and A23 as produced in *E. coli*. K (green and red) represents amino acid lysine. Underlined sequence at the C-terminus shows AviTag containing one lysine (green) used by enzyme BirA to attach a single biotin molecule. His-6 tag for purification and detection purpose at the C-terminus is shown in blue. Dashes (-) indicate gaps introduced for alignment. (For interpretation of the references to color in this figure legend, the reader is referred to the web version of this article.)

Table 1
Properties of VHH M200 analytes. For further explanation see text. n.d.: not determined. w/o: without. K_D: affinity constant.

	Properties of VHH M200 analytes					
	Analyte	Size (kDa)	Epitope	Epitope number per analyte	K_D per antigen (μM)	K_D per epitope (μM)
FMDV (146S)	Intact food-and-mouth disease virus particle	8200, (Vande Woude et al., 1972)	GH-loop	60	0.012	0.72
12S	Pentameric subunits of FMDV	265–282 (Vasquez et al., 1979)	GH-loop	5	0.19	0.98
Peptide PAT49	Synthetic peptide representing residues 136–160 of GH-loop of structural protein VP1	3	Synthetic peptide	1	30	30
BSA–PAT49 (20 equivalents peptide)	Peptide PAT49 coupled to BSA	103	Synthetic peptide	ca. 14	n.d.	n.d.
BSA–PAT49 (5 equivalents peptide)	Peptide PAT49 coupled to BSA	72	Synthetic peptide	ca. 2	n.d.	n.d.
R-phycoerythrin–PAT49	Peptide PAT49 coupled to R-phycoerythrin	n.d. (240 without peptide PAT49)	Synthetic peptide	n.d.	n.d.	n.d

VHH M200 recognizes the foot-and-mouth disease viral particle (FMDV) of the O1 Manisa strain (Harmsen et al., 2007b). For an overview of VHH M200 analytes see Table 1. Intact FMDV particles (8200 kDa) (Vande Woude et al., 1972) are icosahedral and are composed of 60 copies of coat proteins (Fry et al., 2005). VHH M200 is specific for the GH-loop of coat protein VP1 (Harmsen et al., 2007b). Intact FMDV are also referred to as 146S particles based on its sedimentation behavior in sucrose density gradients (Doel and Baccarini, 1981). Mildly acidic conditions were used to breakdown the intact 146S particle into stable 12S particles. 12S particles (265–282 kDa; Vasquez et al. 1979) include 5 copies of VP1 (Sangar et al., 1976), and thus expose 5 epitopic sites for M200 (Vasquez et al., 1979). The 3 kDa small peptide PAT49 (YGDGTVANVRGDLQVLAQKAARALPC), corresponding to amino acid residues 136–160 of the GH-loop of structural protein VP1, represents the epitope of FMDV that is recognized by VHH M200 (Harmsen et al., 2007b). To examine the effect of different analytes on oriented capture molecules, proteins exposing multiple copies of peptide PAT49 were prepared. To this end bovine serum albumin (BSA)–PAT49 and R-phycoerythrin–PAT49 were synthesized by coupling the cysteine-containing peptide PAT49 to maleimide-activated proteins. Maleimide-activated proteins possess more than one maleimide-linker, and the coupling reaction with 5 and 20 M equivalents of peptide

PAT49 results in multiple epitope sites exposing analytes. Size shift of BSA–PAT49 on SDS-PAGE (Fig. 2B) indicated that ca. 14 peptides (20 equivalents PAT49) or 2 peptides (5 equivalents PAT49) were bound per BSA molecule.

3.3. A surface plasmon resonance chip functionalized with uniformly oriented and randomly oriented biotinylated VHHs.

A SPR chip was designed to test the effect of uniform orientation of VHHs on analyte detection. To exclude any influence of the biotinylation of VHH to analyte binding, VHHs were used both in a uniformly oriented and randomly oriented fashion. To this end, two "uniform orientation" flow channels (Fc3 and Fc4; Fig. 1B and D) of a CM5 chip were coated with streptavidin, onto which biotinylated VHH was non-covalently immobilized. The other two "random orientation" flow channels (Fc1 and Fc2; Fig. 1C and D) were functionalized with biotinylated VHHs by covalent carbodiimide chemistry directly onto the CM5 chip, without the use of streptavidin. M200 was immobilized with a uniform orientation in Fc3 and was randomly oriented in Fc1; A23 was immobilized with a uniform orientation in Fc4 and was randomly oriented in Fc2 (Fig. 1D). This set-up allows binding of an analyte sample to uniformly oriented and randomly oriented VHHs in one experiment. To ensure comparability, it was aimed for the same coupling density of VHHs in uniformly oriented and randomly oriented flow channels. Coupling density of antibodies resulted in VHHs immobilized at a level of 3268 ± 391 RU (average of 12 flow channels) over each of the flow channels. To investigate the strength of the different immobilization strategies (covalent versus non-covalent immobilized), repeated cycles of *M. tuberculosis*1 lysate injection and regeneration with 5 µL 10 mM HCl were performed. Non-covalently immobilized VHH (streptavidin–biotin bond) shows a signal loss of 32% after 30 cycles, whereas covalently immobilized VHH (amine group coupled to carboxyl group) shows a signal loss of 10% after 30 cycles (Fig. 3A). In further experiments, binding of analyte was only compared within a cycle rather than between cycles.

3.4. Effect of uniform orientation of capture molecules

3.4.1. VHH A23 binding

To explore the effect of the uniform VHH orientation on analyte binding, different concentrations of analyte were run over all four flow cells of the sensor chip as designed above, using the M200 channels as reference. As expected, *M. tuberculosis*27 lysates showed binding to VHH A23 (Fc2 and Fc4), while negative controls (*M. smegmatis* binding to A23) did not (data not shown). Uniformly oriented VHH A23 showed a signal for *M. tuberculosis*27 lysates that was about five times higher compared to randomly oriented VHH A23 (Fig. 3B).

3.4.2. VHH M200 binding

3.4.2.1. Impact of analyte size. M200 VHH allows us to test the effect of the molecular weight of the analyte (Table 1), as it binds to both FMDV (8200 kDa) and peptide PAT49 (3 kDa). To this end, these analytes of different size were injected over all four flow channels. As expected, FMDV and peptide PAT49 injections showed binding to VHH M200 (Fc1 and Fc3). When binding was compared between the uniform orientation and the random

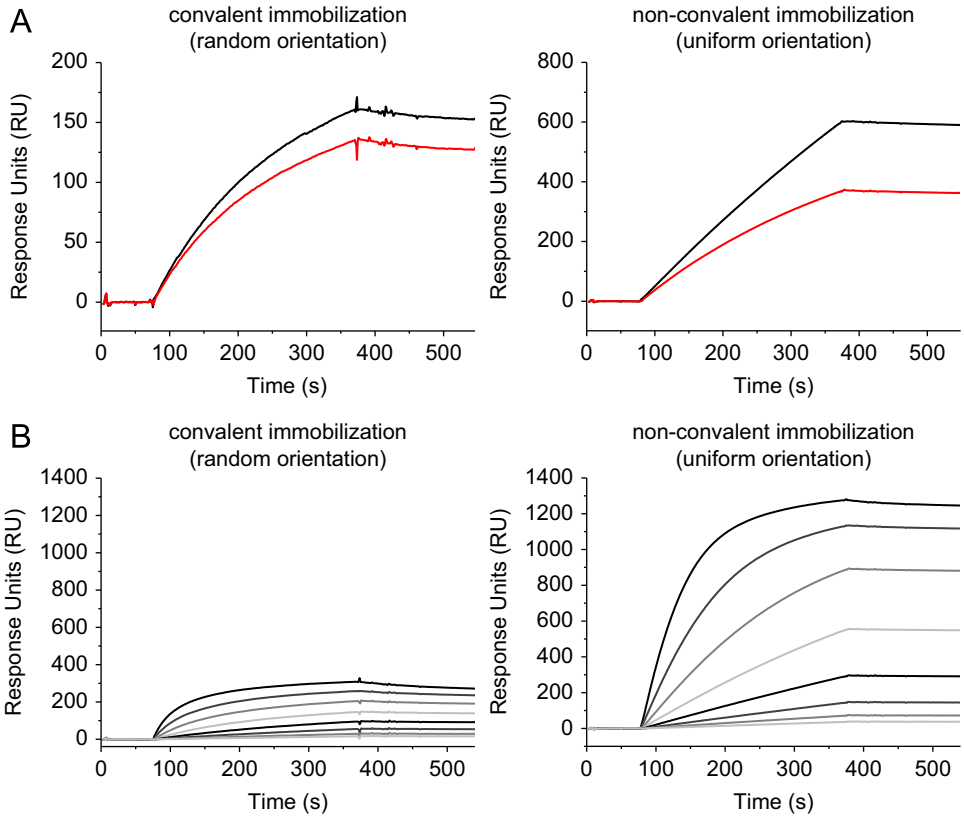

Fig. 3. SPR analysis of A23 capture molecule. A: signal loss of immobilized capture molecules. Samples of *M. tuberculosis*1 lysate (50 µg/mL) were simultaneously analyzed on covalent (left panel) and non-covalent (right panel) immobilized channels, before (black) and after (red) 30 cycles of binding and regeneration by 5 µL 10 mM HCl. B: signal increase on uniformly oriented capture molecules. Samples of *M. tuberculosis*27 lysate (50 µg/mL) were simultaneously analyzed on randomly oriented (left panel) and uniformly oriented (right panel) channels. Samples contained increasing concentrations of analyte (0.4×10^3, 0.8×10^3, 1.6×10^3, 3.1×10^3, 6.3×10^3, 12.5×10^3, 25×10^3 and 50×10^3 ng protein/mL). (For interpretation of the references to color in this figure legend, the reader is referred to the web version of this article.)

orientation, orientation yielded a two-fold higher binding of intact FMDV particles (Fig. 4A). Surprisingly, detection of viral peptide PAT49 benefited much stronger from orientation: a 14 times higher signal was observed when VHHs were uniformly oriented (Fig. 4B).

To investigate the relation between analyte molecular weight and observed signal difference, 12S particle (265–282 kDa) and R-phycoerythrin–PAT49 (240 kDa without peptide PAT49) (Table 1) were injected over all four flow channels. Although the molecular weight of both analytes is similar, only detection of R-phycoerythirin–PAT49 benefited from orientation: a 55 times higher signal was observed when VHHs were uniformly oriented (Fig. 4C and D).

3.4.2.2. Impact of avidity. Comparison of analytes with similar size (R-phycoerythrin and 12S) showed a strong difference in signal increase upon using a uniform orientation of VHHs (Fig. 4C and D), suggesting that other parameters caused the observed signal difference. Another analyte property influencing the binding behavior between analyte and VHH is avidity. Avidity is used to describe the combined binding strength of multiple bond interactions, while affinity is used to define the strength of individual bonds. By the presence of several epitope copies on an analyte, a high apparent affinity will be observed, due to avidity effects. Peptide PAT49 represents a monomeric analyte, whereas FMDV and 12S particles display multiple epitope copies (60 and 5, respectively; Table 1). The influence of avidity on the signal increase was investigated by injecting various concentrations of BSA–PAT49 (ca. 14 peptides PAT49 per binding unit) and 12S particles (5 GH-loops per binding unit) over all four flow channels. Control experiments using BSA-Cys showed no binding onto any of the channels (data not shown), while both 12S particles and BSA-PAT49 showed binding to VHH M200 (Fc1 and Fc3), but did not bind to reference VHH A23 (Fc2 and Fc4) (data not shown). For 12S particles only weak increases in signal (1–1.3-fold) could be observed for the uniformly oriented channel (Table 2). For BSA–PAT49 containing 14 peptides, on the other hand, large increases in signal intensity (21–27-fold) were consistently observed in the uniformly oriented channel (Table 2) over a range of analyte concentrations. Decrease of peptide number in BSA–PAT49 (2 peptides PAT49 per binding unit) lead to a stronger increase in signal intensity for the uniformly oriented VHH (170–227-fold, Table 2).

3.4.2.3. Affinity of analyte. To study the differences of analytes (natural analyte versus peptide PAT49), affinity of M200 was investigated by ELISA (Hutsell et al., 2010). Observed affinity constants (KD) are shown in Table 1. The KD of M200 for the viral derived analytes (FMDV and 12S) was 15-fold lower than the KD value for the peptide PAT49 analyte.

4. Discussion

The experiments performed in the current work for the first time highlight the importance of specific analyte properties on the effect of uniform orientation of the capture molecule (Table 2; Fig. 3B and Fig. 4). Uniform orientation of the M200 VHH affects the binding efficiency of nearly all analytes, but the range of enhancement is rather large: from a hardly noticeable increase by a factor 1.3 to a large 227-fold increase.

The M200 VHH that were immobilized in randomly and uniformly oriented ways allowed us to investigate binding properties of a collection of analytes, which differ in properties such as molecular weight, number of epitopes and affinity.

Our initial hypothesis was that the size of the analyte is important for the effect of uniform orientation. An experiment comparing peptide PAT49 to FMDV particles suggested this (Fig. 4A and B).

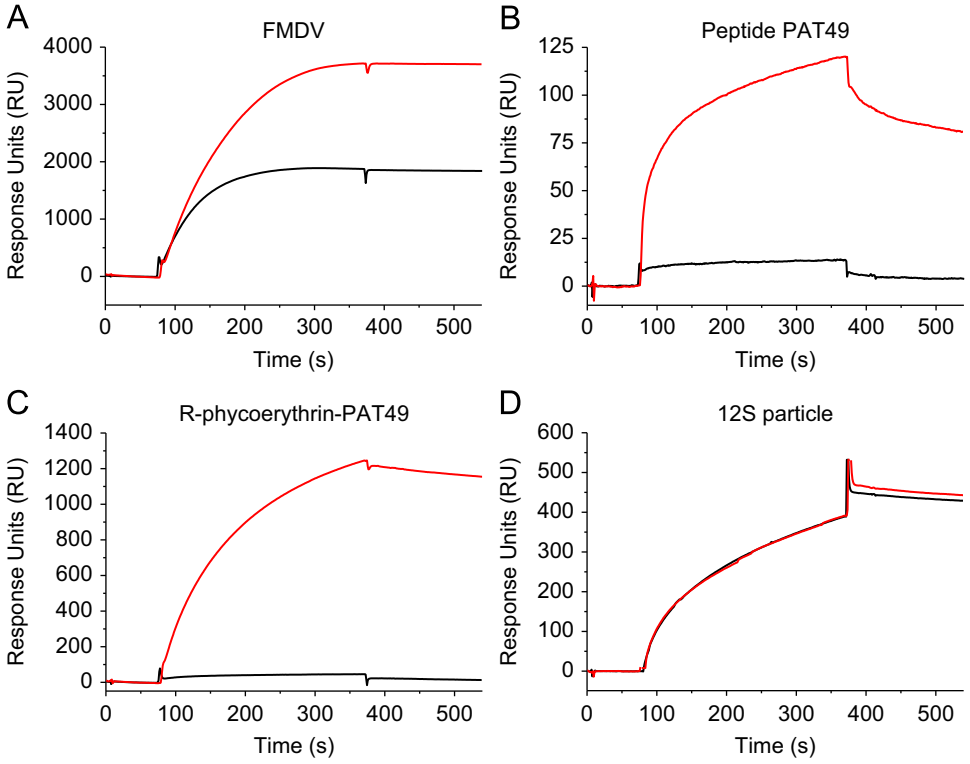

Fig. 4. Signal increase by orientation of M200 for analyte with different molecular weight. Sensorgrams obtained after injection of 12.5 μg/mL FMDV (A), 1.25 μg/mL peptide PAT49 (B), 50 μg/mL R-phycoerythrin–PAT49 (C) and 40 μg/mL 12S particle (D). Signal measured by randomly oriented M200 shown in black, measured by uniformly oriented M200 shown in red. (For interpretation of the references to color in this figure legend, the reader is referred to the web version of this article.)

Table 2
Improvement factor of binding signal obtained by orientation of capture molecule M200. Signal obtained after injection of analyte at indicated concentration. Signal was measured as response unit (RU) 30 s after injection was stopped. Improvement factor was calculated by dividing the signal of uniformly oriented VHH M200 by the signal of randomly oriented VHH M200.

Concentration analyte (in μg/mL)	SPR signal of randomly oriented M200 (in RU)	SPR signal of uniformly oriented M200 (in RU)	Improvement factor
FMDV (8200 kDa)			
12	1854	3712	2
Peptide PAT49 (3 kDa)			
1	10	138	14
R-phycoerythrin–PAT49 (240 kDa without peptide)			
50	22	1208	55
12S particle (265–282 kDa)			
40	446	464	1.0
20	345	345	1.0
5	310	406	1.3
BSA–PAT49 (103 kDa)			
50	28	763	27
25	31	695	22
12	29	622	21
6	23	598	26
3	18	521	29
BSA-PAT49 (72 kDa)			
50	3	508	170
25	2	454	227
12	2	366	183

Peptide PAT49 binding to randomly oriented M200 resulted in a 14 times lower binding signal compared to uniformly oriented M200, whereas the effect of orientation was modest for analyte FMDV. Peptide PAT49 (3 kDa) is about 6 times smaller than M200 (18 kDa) and therefore diffuses more efficiently through the dextran layer covering the CM5 SPR chip, binding to all accessible VHHs on the surface. This suggests that 14 times less VHHs are available for analyte binding in the random orientation. Larger analytes, however, can affect binding by lateral packing leading to a lower amount of captured analyte. Tested FMDV, with a mass of 8200 kDa and a diameter of 25 nm (Grubman and Baxt, 2004), represents such a big analyte. Orientation of capture molecules showed only a modest signal increase for FMDV, which might be caused by molecular weight-related factors, such as steric hindrance, shielding neighboring capture molecules upon analyte binding, and a limitation in the capacity to penetrate the dextran layer. The effect of size should be negligible when 12S particles were compared with R-phycoerythrin–PAT49. Both have similar sizes (Table 1), and would benefit in a similar way from uniform orientation. Surprisingly, however, R-phycoerythrin–PAT49 showed an enormous, 55-fold signal increase upon uniform orientation of the M200 VHHs, while 12S particles did not show any such effect (Fig. 4C and D, Table 2). Therefore other explanations for differences in the effect of uniform orientation were investigated.

A second explanation for differences in the effect of uniform orientation was possibly epitope avidity. Avidity, which reflects the combined binding strength of multiple analyte-antibody interactions, could depend on many factors: e.g. capture molecule density, flexibility of antibody, analyte, dextrane layer and the availability of free antibodies. We tried to find consistent effects of the number of epitopes. In SPR, analyte bound to one capture molecule gives the same signal as an analyte bound via several capture molecules. However, binding to multiple capture molecules leads to stabilization of the analyte-antibody complex on the chip and shifts the equilibrium constant (Pukin et al., 2007). To examine the relation of analyte–avidity and signal increase by uniform orientation, proteins varying in the number of exposed epitopes were compared, but no consistent relationship between epitope number and effect of orientation could be observed.

Comparing intact FMDV (60 GH-loop epitopes) and 12S particles (5 GH-loop epitopes), only a slight effect could be observed, showing that more epitopes would lead to a somewhat stronger effect of orientation (Table 2). On the other hand, the comparison of BSA–PAT49 carrying 14 or 2 peptide epitopes suggests an opposite effect: BSA–PAT49 carrying 14 epitopes showed $\pm$25-fold higher binding by orientation, whereas BSA–PAT49 carrying only 2 epitopes showed a $\pm$200-fold increase in signal. The monomeric PAT49 peptide by itself, showed again a 14-fold improved signal by orientation. Apparently there is not a straightforward relationship between the number of epitopes and the effect of orientation.

The experiments presented in this work indicate that the effect of uniform orientation is much higher on peptide PAT49 and its protein conjugates (BSA–PAT49 and R-phycoerytrin–PAT49), compared to virus-derived analytes such as FMDV and 12S. In fact, the results in Fig. 4 suggest that the binding of PAT49-containing analytes is hampered on non-oriented M200 VHH. Possibly, the chemistry used for random immobilization could result in a bias towards wrongly-oriented capture molecules. For random orientation, covalent cross-linking between free, accessible primary amines of biotinylated VHH and the carboxyl group on the CM5 surface was used. Primary amines are usually outward-facing in the protein due to its positive charge under physiological conditions (Hermanson, 2008), and therefore are accessible for conjugation. VHHs can be immobilized via the ε-amines, present in lysine side chains, or via the α-amine, present at the N-terminus of the protein. Biotinylated M200 contains 8 lysine side chains and A23 contains 7 available lysine side chains (Fig. 2C), therefore multiple orientations during immobilization are possible via ε-amines. However, due to its lower pK value, the reactivity of the N-terminal amino group is about 300 times higher than that of amino groups of lysine side-chains (Hernandez and Fernandez-Lafuente, 2011). The N-terminus of VHHs is located close to the analyte binding site. Therefore, the use of the standard, non-oriented immobilization method could result in a situation where more VHHs are immobilized "up-side down" via the N-terminal α-amine in the non-orientated immobilization method than by the ε-amines present in lysine side chains. However, a predominant "up-side down" orientation of VHH would not explain why PAT49-containing analytes would bind more poorly, while this seems not to be the case for the more bulky FMDV and 12S analytes. Possibly, the configuration of the binding site affects binding behavior more strongly than avidity or size. The epitope amino acids as they occur in peptide PAT49 are probably not in their natural analyte environment. Therefore they may adopt a configuration that differs from the native (virus) configuration, which may lower the affinity of VHH M200. Indeed it was previously reported that the peptide conformation plays a crucial role in antibody-analyte interaction (Gomes et al., 2001). The GH-loop forms a highly flexible, disordered protrusion of structural protein VP1 on the virus surface, but synthetic GH-loop peptides introduced into carrier molecules showed that stabilization of the loop is dependent on contacts of neighboring regions (de Prat-Gay, 1997; Feliu et al., 1998). Therefore the affinity of M200 should differ between investigated analytes. Indeed, the affinity for peptide PAT49 was lower than for the analytes FMDV and 12S, suggesting that affinity of analytes has an effect in the tested set-up. Also Peluso et al. (Peluso et al., 2003) suggested that affinity might play a major role when low concentrations of analyte were used.

In all cases studied here, the uniform orientation of capture molecules leads to improvements of signal, both for the A23 and

the M200 VHH. Although the extent to which orientation results in signal improvement differed. The differential effect of uniform orientation on signal intensity between different capture molecules has been well documented. Many studies have been performed using staphylococcal protein A to orient antibodies, and have demonstrated clear effects of orientation on immunoassay sensitivity (e.g. Tajima et al., 2011). Peluso et al. compared randomly biotinylated and site-specifically biotinylated capture molecules (immunoglobulins and Fab fragments), using three different antibodies, and observed 1.6–10-fold improvements, depending on the capture molecule (Peluso et al., 2003). In their work, the orientation was mediated by either site-specific or random biotinylation. A study carried out on VHHs in a set-up very similar to ours, site-specific biotinylation showed a slightly decreased level of detection compared to VHHs that were randomly immobilized via the primary amines (Saerens et al., 2005). Similar to our set-up, Saerens et al., (2005) used the C-terminus to introduce the biotin moiety by BirA enzyme leading to unique probe biotinylation at the antipode of the analyte binding site. One of the explanations for the difference between the two studies could be that the human prostate-specific analyte, which was used in their study, has properties that do not favor recognition by uniformly oriented VHH. Another explanation could be that the rigid human IgA-1 hinge deployed by Saerens et al. between the VHH and the AviTag interfered with correct orientation, while the flexible glycine-rich linker deployed in this study (Fig. 2C) would permit a correct orientation.

5. Conclusion

In the current work we show that analyte properties can have a large impact on biosensors signals when uniformly oriented and randomly oriented capture molecules are used. Orientation effects up to a factor 227 have been measured, and the observed range of orientation effects (factor 1.3–227) was analyzed with respect to a series of analyte properties. While size and avidity effects do not seem to give a systematic improvement factor, the strength of the interaction dominates the effect of orientation of the antibody: weaker interactions benefit much more from uniform orientation than stronger interactions. Clearly, this steers the further research that is needed into the effect of capture molecule orientation on sensing of target and non-target analytes.

Acknowledgments

This work was funded by the European Union through the Marie Curie Integrated Training Network project Hierarchy (contract: PITN-2007-215851) and the IPOP (Instellings Plan/Ontwikkelings Plan)-Bionanotechnology program, a Wageningen UR strategic research program running from 2008–2011. Sponsors had no influence in study design; collection, analysis, and interpretation of data; in the writing of the report; and in the decision to submit the paper for publication. The help and suggestions made by Dr. Maarten Jongsma and Dr. Willem Haasnoot are kindly acknowledged. The authors also like to thank Saurabh Kumar Srivastava for preparation of VHH constructs.

References

Baio, J.E., Cheng, F., Ratner, D.M., Stayton, P.S., Castner, D.G., 2011. Journal of Biomedical Materials Research Part A 97A (1), 1–7.
Balevicius, Z., Ramanaviciene, A., Baleviciute, I., Makaraviciute, A., Mikoliunaite, L., Ramanavicius, A., 2011. Sensors and Actuators B: Chemical 160 (1), 555–562.
Beckett, D., Kovaleva, E., Schatz, P.J., 1999. Protein Science 8 (4), 921–929.
Cho, I.-H., Paek, E.-H., Lee, H., Kang, J.Y., Kim, T.S., Paek, S.-H., 2007. Analytical Biochemistry 365 (1), 14–23.
Cho, I.-H., Park, J.-W., Lee, T.G., Lee, H., Paek, S.-H., 2011. Analyst 136 (7), 1412–1419.
Cho, I.-H., Seo, S.-M., Jeon, J.-W., Paek, S.-H., 2009. Journal of Biomedicine and Biotechnology , http://dx.doi.org/10.1155/2009/104094.
Cloutier, S.M., Couty, S., Terskikh, A., Marguerat, L., Crivelli, V., Pugnieres, M., Mani, J.C., Leisinger, H.J., Mach, J.P., Deperthes, D., 2000. Molecular Immunology 37 (17), 1067–1077.
de Prat-Gay, G., 1997. Archives of Biochemistry and Biophysics 341 (2), 360–369.
Doel, T.R., Baccarini, P.J., 1981. Archives of Virology 70 (1), 21–32.
Dumoulin, M., Conrath, K., Van Meirhaeghe, A., Meersman, F., Heremans, K., Frenken, L.G.J., Muyldermans, S., Wyns, L., Matagne, A., 2002. Protein Science 11 (3), 500–515.
Farris, L.R., McDonald, M.J., 2011. Analytical and Bioanalytical Chemistry 401 (9), 2821–2829.
Feliu, J.X., Benito, A., Oliva, B., Avilés, F.X., Villaverde, A., 1998. Journal of Molecular Biology 283 (2), 331–338.
Fry, E., Stuart, D., Rowlands, D., 2005. Current Topics in Microbiology and Immunology 288, 71–101.
Gomes, P., Giralt, E., Andreu, D., 2001. Vaccine 19 (25–26), 3459–3466.
Grubman, M.J., Baxt, B., 2004. Clinical Microbiology Reviews 17 (2), 465–493.
Harmsen, M.M., Fijten, H.P.D., Dekker, A., Eble, P.L., 2008. Veterinary Microbiology 132 (1–2), 56–64.
Harmsen, M.M., Fijten, H.P.D., Dekker, A., Eblé, P.L., 2007a. Proceedings of the First Annual Meeting EPIZONE "EPIZONE INSIDE OUT", May 30th–June 1st 2007, Lublin, Poland.
Harmsen, M.M., Fijten, H.P.D., Westra, D.F., Coco-Martin, J.M., 2011. Vaccine 29 (15), 2682–2690.
Harmsen, M.M., van Solt, C.B., Fijten, H.P.D., van Keulen, L., Rosalia, R.A., Weerdmeester, K., Cornelissen, A.H.M., De Bruin, M.G.M., Eble, P.L., Dekker, A., 2007b. Veterinary Microbiology 120 (3–4), 193–206.
Hermanson, G.T., 2008. Bioconjugate Techniques 2nd edition.
Hernandez, K., Fernandez-Lafuente, R., 2011. Enzyme and Microbial Technology 48 (2), 107–122.
Holford, T.R.J., Davis, F., Higson, S.P.J., 2012. Biosensors and Bioelectronics 34 (1), 12–24.
Hutsell, S.Q., Kimple, R.J., Siderovski, D.P., Willard, F.S., Kimplec, A.J., 2010. Methods in Molecular Biology 627, 75–90.
Klonisch, T., Panayotou, G., Edwards, P., Jackson, A.M., Berger, P., Delves, P.J., Lund, T., Roitt, I.M., 1996. Immunology 89 (2), 165–171.
Le Brun, A.P., Holt, S.A., Shah, D.S.H., Majkrzak, C.F., Lakey, J.H., 2011. Biomaterials 32 (12), 3303–3311.
Park, J.W., Cho, I.H., Moon, D.W., Paek, S.H., Lee, T.G., 2011. Surface and Interface Analysis 43 (1-2), 285–289.
Peluso, P., Wilson, D.S., Do, D., Tran, H., Venkatasubbaiah, M., Quincy, D., Heidecker, B., Poindexter, K., Tolani, N., Phelan, M., Witte, K., Jung, L.S., Wagner, P., Nock, S., 2003. Analytical Biochemistry 312 (2), 113–124.
Pukin, A.V., Branderhorst, H.M., Sisu, C., Weijers, C.A.G.M., Gilbert, M., Liskamp, R.M.J., Visser, G.M., Zuilhof, H., Pieters, R.J., 2007. ChemBioChem 8 (13), 1500–1503.
Renisio, J.-G., Pérez, J., Czisch, M., Guenneugues, M., Bornet, O., Frenken, L., Cambillau, C., Darbon, H., 2002. Proteins 47 (4), 546–555.
Saerens, D., Frederix, F., Reekmans, G., Conrath, K., Jans, K., Brys, L., Huang, L., Bosmans, E., Maes, G., Borghs, G., Muyldermans, S., 2005. Analytical Chemistry 77 (23), 7547–7555.
Saerens, D., Huang, L., Bonroy, K., Muyldermans, S., 2008. Sensors 8 (8), 4669–4686.
Sangar, D.V., Rowlands, D.J., Cavanagh, D., Brown, F., 1976. Journal of General Virology 31 (1), 35–46.
Sarma, V.R., Silverton, E.W., Davies, D.R., Terry, W.D., 1971. Journal of Biological Chemistry 246 (11), 3753–3759.
Seo, M.-H., Han, J., Jin, Z., Lee, D.-W., Park, H.-S., Kim, H.-S., 2011. Analytical Chemistry 83 (8), 2841–2845.
Shen, G., Cai, C., Wang, K., Lu, J., 2011. Analytical Biochemistry 409 (1), 22–27.
Song, H.Y., Zhou, X., Hobley, J., Su, X., 2012. Langmuir 28 (1), 997–1004.
Spinelli, S., Frenken, L., Bourgeois, D., Ron, L.d., Bos, W., Verrips, T., Anguille, C., Cambillau, C., Tegoni, M., 1996. Nature Structural Biology 3, 752–757.
Tajima, N., Takai, M., Ishihara, K., 2011. Analytical Chemistry 83 (6), 1969–1976.
Thomassen, Y.E., Meijer, W., Sierkstra, L., Verrips, C.T., 2002. Enzyme and Microbial Technology 30 (3), 273–278.
Trilling, A.K., de Ronde, H., Noteboom, L., van Houwelingen, A.l., Roelse, M., Srivastava, S.K., Haasnoot, W., Jongsma, M.A., Kolk, A., Zuilhof, H., Beekwilder, J., 2011. PLoS ONE 6 (10), e26754 1–10.
Vande Woude, G.F., Swaney, J.B., Bachrach, H.L., 1972. Biochemical and Biophysical Research Communications 48 (5), 1222–1229.
Vareiro, M.M.L.M., Liu, J., Knoll, W., Zak, K., Williams, D., Jenkins, A.T.A., 2005. Analytical Chemistry 77 (8), 2426–2431.
Vashist, S.K., Dixit, C.K., MacCraith, B.D., O'Kennedy, R., 2011. Analyst 136 (21), 4431–4436.
Vasquez, C., Denoya, C.D., La Torre, J.L., Palma, E.L., 1979. Virology 97 (1), 195–200.
Zeng, X., Shen, Z., Mernaugh, R., 2012. Analytical and Bioanalytical Chemistry, 1–12.